International Journal of Engineering and Geosciences
https://dergipark.org.tr/en/pub/ijeg
e-ISSN 2548-0960

The effect of DEM resolution on topographic wetness index calculation and visualization: An insight to the hidden danger unraveled in Bozkurt in August, 2021

Arif Oguz Altunel[*1]

[1]*Kastamonu University, Faculty of Forestry, Forest Engineering, Türkiye*

Keywords
Global DEMs
Quad maps
DEM resolution
TWI
Flood

Research Article
DOI: 10.26833/ijeg.1110560

Received: 28.04.2022
Accepted: 24.07.2022
Published: 19.10.2022

Abstract

Topographic Wetness Index, also known as the compound topographic index, (TWI) is a topographic indicator that calculates the potential of where water is likely to accumulate during excessive precipitation cycles resulting from abrupt atmospheric anomalies. High index values represent serious potential of water accumulation due to low slope, and the opposite for high slope. As expected from the term, slope, Digital Elevation Model (DEM) datasets play an important role in the calculation of TWI. DEMs are produced utilizing tachometry, GPS benchmarking, UAV, aerial or satellite image capture and LIDAR capabilities. However, no matter how it is generated, a DEM is as good as the actual ground sampling algorithm, on which the final resolution is based. Using six different DEM resolutions coming from three global and one national source presented in three different setting coverages, upper feeder basin of Bozkurt sub-province, Kastamonu, was analyzed emphasizing the urbanized part of the sub-province, which was devastated during the August 11th, 2021 flood. Coarser resolution missed the overall precision while the finer resolution captured it nicely. On the flip side, finer resolution excessively fragmented the questioned area while the coarser resolution formed a unity coinciding with the destructed area recorded during the event.

1. Introduction

Habitation on the Turkish Black-sea coast dates back quite some time. Due to the morphological structuring of the topography, which the mountains run parallel to the coast line, many provinces and sub-provinces have settled on or near the coast line, which have provided easy access to sea, warmer climate year-round and nicer aesthetics to be around. However, this living preference had a catch from time to time. Each and every urbanized location on Black-sea coast has experienced floods and landslides varying in severity during their existence [1-2]. The reason for the devastations has resulted from the fact that the towns situated at and around sea-bound discharge paths of docile looking waterways, are swept out to sea causing immense property damage and death along with the surging water coming fully loaded down from the feeder basins, aka upper watersheds [3]. Alluvial fans between the feeder basins and the sea are where the surging water is dispersed losing its destructive energy during heavy rains before converging with the sea. When towns are situated on them, they are in danger to some degree because the feeder basins can only collect and convey a certain amount of water during such events [4]. However, when towns are situated right at the mouth of the feeder basins, where topography is still not tame enough for the hurdling downward water, the damage becomes proportionately high because man made infrastructures cannot withstand against that much force. One such sub-province, Bozkurt, of Kastamonu was hit by a record-breaking rain storm in August 11th, 2021 when the majority of the town was run down by the rushing waters coming from its feeder basin. Along with the neighboring two other sub-provinces, property damage and death toll were unprecedented.

In the scope of this study, a frequently used hydrology indices, topographic wetness index, which has been known as an indicator for determining the places inherently keeping water accumulation potential, through a raster surface [5-6], was evaluated. Reliably forecasting soil moisture patterns in landscapes was a serious challenge in the past so that many notable occurrences cost considerable property damage and death all across the Earth [7-10]. TWI was first developed

* **Corresponding Author**
*(aoaltunel@kastamonu.edu.tr) ORCID ID 0000-0003-2597-5587

Cite this article
Altunel, A. O. (2023). The effect of DEM resolution on topographic wetness index calculation and visualization: An insight to the hidden danger unraveled in Bozkurt in August, 2021. International Journal of Engineering and Geosciences, 8(2), 165-172

by physically basing on a runoff model, TOPMODEL, which ran with the assumption that the hydraulic slope could be estimated by the topographic slope [11]. It has lately been accepted as a powerful measure in defining flood preparedness scenarios [12-13]. The index specializes in rainfall runoff predictions and spatial soil moisture and water accumulation simulations [14]. Six different DEM datasets, three from global sources and one displayed in three different visualization settings, from Turkish national quad map coverage of 2010, were used to delineate Bozkurt feeder basin to see how DEM resolution can differ and can help specify residential flood risk areas during heavy rain storms.

2. Materials and Methodology

2.1. Study area

Bozkurt is one of six Black Sea bound sub-provinces of Kastamonu. It has typical Black Sea topography and morphological characteristics (Figure 1) along with lush deciduous and coniferous forests managed by the Turkish forest service. Although considered as a coastal town, its residential part extends inland along its docile looking creek/stream, so that the neighboring sub-province Abana sits directly on the alluvial fan of Bozkurt's feeder basin. Sub-province's neighborhoods, recreation infrastructure and commercial districts are all situated immediately around the stream channel, which was overwhelmed by the deluge coming from the feeder basin on August 11th, 2021. Compared to the neighboring ones, it has a rather small feeder basin of 11851.5 ha whereas Catalzeytin had 31252 ha and Ayancik had 59081 ha. Considerable property damage and human loss also occurred in these mentioned sub-provinces, however what Bozkurt experienced was beyond comprehension. That's why it is singled out for analysis in this study.

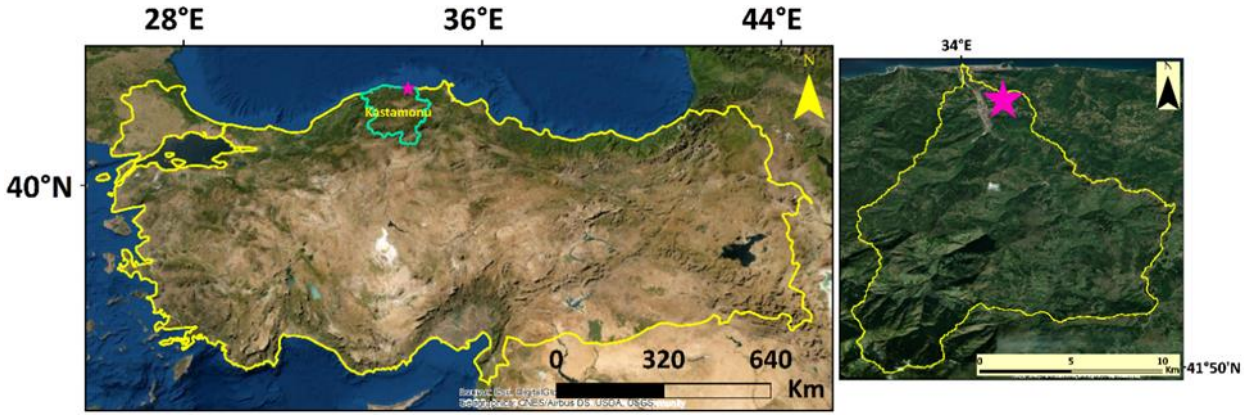

Figure 1. Location of Bozkurt sub-province and its feeder basin

2.2. Methodology

Three different-resolution global DEM datasets, ALOS PALSAR, 12.5 m [15], AW3D30, 30 m [16] and TanDEM-X, 90 m [17] were acquired from their respective geo-portals. ALOS PALSAR and TanDEM-X DEMs were respectively produced with the capabilities of L-band and X-band Synthetic Aperture Radar (SAR) interferometric techniques [18-19] whereas the initial and the successive releases of AW3D30 DEM have been produced with panchromatic optical sensor (PRISM) captured stereo image processing [20-21]. Many studies have surfaced questioning and validating their effectiveness and practicality in various fields of studies [22-26]. All three DEM datasets were positioned defining Universal Transverse Mercator projection over World Geodetic System, 1984 horizontal datum under Bozkurt feeder basin polygon. 34 m Geoid height [27] was deducted from ALOS-PALSAR DEM [28].

Besides, three more DEM datasets were produced from vectorized and 1:25000 scaled national quad maps [29]. First, four such maps were simultaneously tied together to form an initial Triangulated Irregular Network (TIN) surface. Then, a TIN to raster conversion was carried out accepting the default resolution(s), 104 m. Second, all maps were clipped by Bozkurt feeder basin polygon (Figure 2), the clipped parts were tied together and a second TIN surface was generated expecting a tighter GRID pattern. When the conversion was again applied, the result indeed produced a better resolution, 67 m. No resampling algorithm was applied in achieving these figures in either case.

National quad map(s) which have been produced via photogrammetric capabilities, solely relying on stereo air-photo capture, depict the stationary topography of a region in a medium scale. Accepted as a reasonable scale by many nations [30-31], they include contour lines following the natural formation of the terrain. Contour intervals widens in distance due to subtle elevation differences in flat areas whereas they come tightly together as topography becomes treacherous, accentuating the elevation in short distances [32]. This uneven, non-systematic elevation distribution within quad maps is the reason behind their DEM generation performance. Since TIN algorithm uses these contour lines to form a surface, it changes in precision when the area of interest shifts, even within the same map(s) as well as in the subsequently produced raster model(s). No one quad map depending surface model distinctness is the same as another. This is how two initial different raster models given above, were produced from the same number of national quad maps (Table 1). Additionally, a

resampled DEM derived from the same national quad map(s) was also produced while converting from TIN, specifying a 30 m cell size. A total of six DEM datasets with different resolutions were individually subjected to "Topographic Wetness Index" algorithm to see how DEM resolutions would differ, and which one would approximate the extend of the heavily damaged area devastated in Bozkurt sub-province in August 11th, 2021. All analyses were performed using ArcGIS 10.8.

Table 1. Specifications of the directly used and produced DEM datasets

DEM Source	Production type	Resolution (m)	Maker	Availability
ALOS_PALSAR	L-band SAR	12.5	JAXA	https://search.asf.alaska.edu/#/?dataset=ALOS
AW3D30	Stereo Image	23.18	JAXA	https://www.eorc.jaxa.jp/ALOS/en/aw3d30/data/index.htm
TanDEM-X	X-band SAR	80.7	DLR	https://download.geoservice.dlr.de/TDM90/
National Quad-cut	Aerial stereo photography	67	General Directorate of Mapping	upon institutional request
National Quad-whole		104		
Resampled nat. quad.		30		

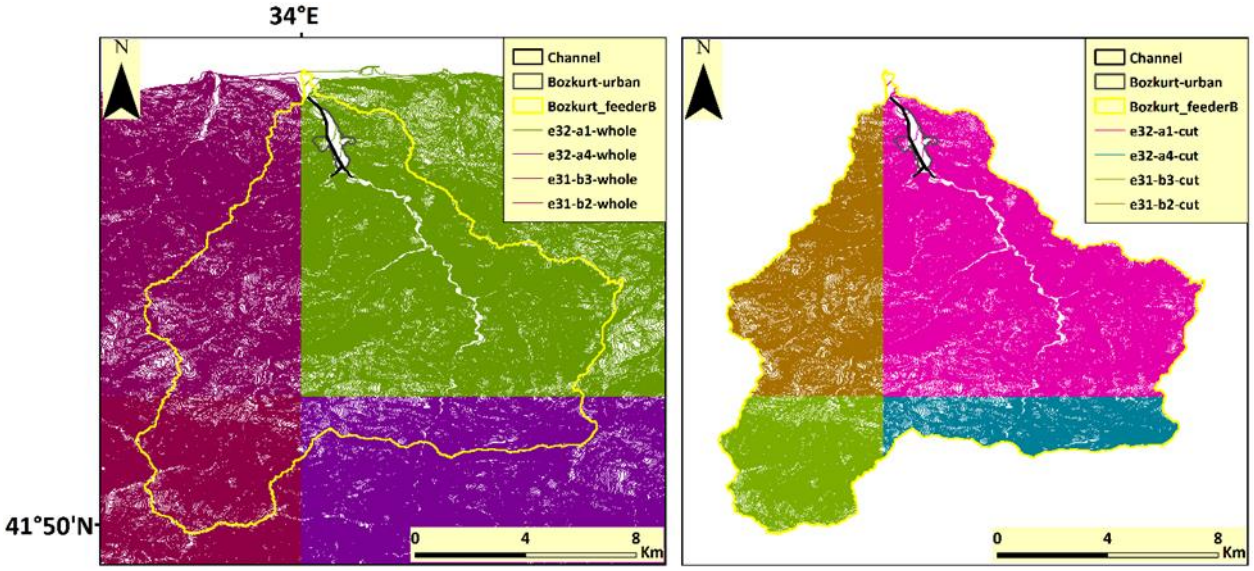

Figure 2. Start of surface generation scheme from vectorized quad maps as whole vs. cut

2.3. Topographic Wetness Index Algorithm and calculation progress on a raster

TWI is an algorithm which is frequently addressed in hydrology driven studies [33-34]. It can be applied on any DEM no matter what its resolution is because DEM resolution is the driving factor behind the successful generation of TWI. The practicality of knowing where water might accumulate at unexpected times, also translate to where water might be sought after in case of need because every water droplet accumulated during rain surely feeds the ground water in the long run. Figure 3 shows how TWI is calculated starting from the initial DEM input.

Through this algorithm, elevation embedded raster DEM cells are transformed into water accumulation risk bearing values ranging from less than 0 to 30 [13]. High index values would indicate high potential of water accumulation due to low slope and vice versa. To find a better TWI producing DEM performance, a hypothetical threshold value, which was applied to all six TWI results, was set. Thus, flood plain acreages were calculated, classifying the TWI results elaborating over this threshold value of more than or equal to "10". Total count of raster cells with TWI values of "10 ≤" was multiplied with the square of the respected raster cell size to achieve the acreages within flood plain (*-fld pln) designated blue polygon in Figure 4. TWI is a unique tool allowing users, decision makers and planners to identify areas which have the potential of getting adversely affected by water accumulation or flooding during excessive rainfall scenarios. Thus city planners can benefit from its visual mechanism in residential site selection and preventive vegetative or afforestation initiatives. Six different resolution DEMs, i.e., three obtained from open-access geo-portals and three manufactured from national quad map coverages, were used to produce TWIs for Bozkurt sub-province of Kastamonu.

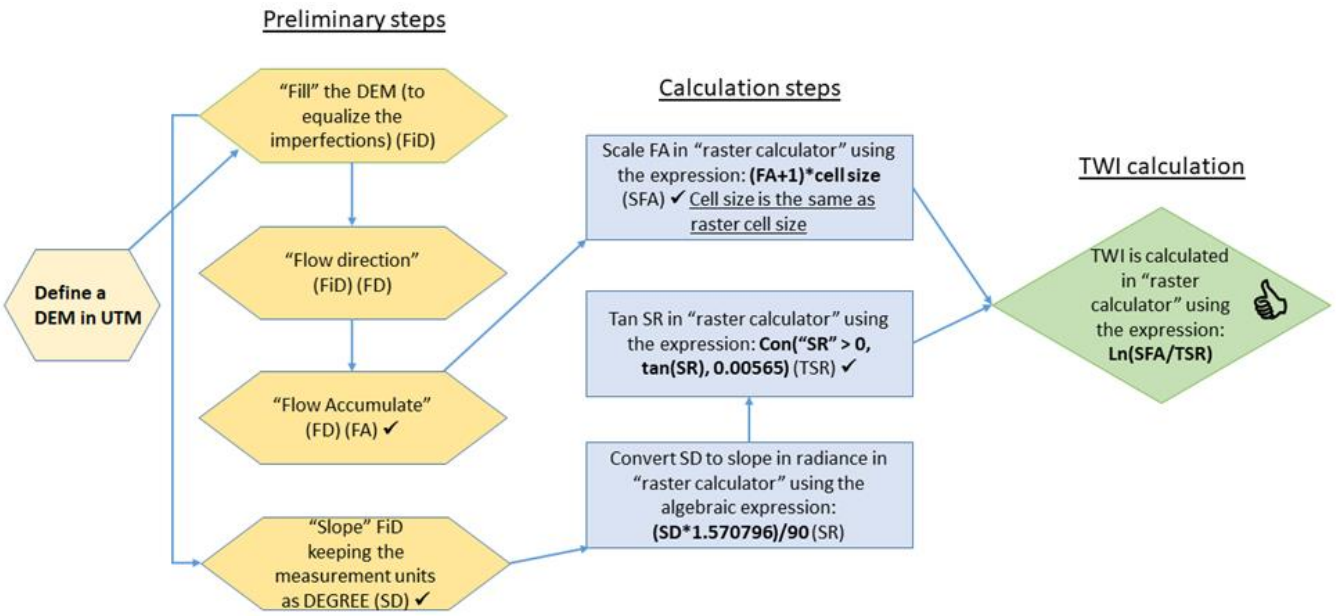

Figure 3. Sequence of turning a DEM into calculated TWI surface

3. Results and Discussion

DEM resolution is important for topographic visualization if intricate work is required. As of today, the highest precision is acquired through LIDAR [35-37] although there are other possibilities, i.e., UAV, air-borne or space-borne image capture derived site specific or large-scale DEM productions, varying in degree of accuracy [29, 38-39]. However, highest precision is not always the sought after or guaranteed requirement obtained from a DEM [40-41]. In an attempt to find suitable flood inundation maps for places where high resolution DEM datasets were not available, Saksena and Merwade [42] unearthed the fact that coarser resolution DEM datasets can provide reliable and improved maps. Quad map extracted inserts in Figure 4 appeared to display better areal distributions compared to much higher resolution ALSO-PALSAR and AW3D30 DEM derived fragmented looking ones. Jeon et al. [43] stated that channel slope became steeper as DEM resolution increased. Although this was a conclusion derived from a simulation, it might very well be one of the underlying factors in real-time feeder basin dynamics of Bozkurt sub-province (Figure 4) because given its small size, 11852 ha, the precipitation falling inside feeder basin swiftly descended into the city and wreak havoc especially on flood plain designated area (blue polygon). Hancock [44] mentioned that hillslope and hydrological details would be lost when larger than 10 m DEM resolutions are used. Similarly, this study also confirmed that topographical detail would be lost from the low resolution onward simply because minute slope differences are aggregated into larger surfaces as the DEM resolution is increased, however this situation obviously did not tarnish the fact that quad map derived inserts in Figure 4 produced comparably better inundation scenarios compared to Global DEM derived results [45].

Although the analyses were performed on the Bozkurt feeder basin's entirety, the emphasize was given to the residential part of the sub-province because the damage mostly concentrated in this part (Figure 4). As the DEM resolution increased, the practicality of the visualization started losing its appeal. ALOS-PALSAR DEM calculated TWI which comparatively provided the highest resolution in this study, indicated almost a no-development area right within the present-day Bozkurt residential extent concentrating around the channel apparent from the water indicating blue-patchy looking pixels in the respectable insert in Figure 4. Nevertheless, this high resolution captured so much detail that it lost the complete picture, thus the insert showed only partial risk as if the rest was secure to settle within the flood plain. The east and west wings of the area were not as heavily risky as the rest of the extent because those were the suburbs erected on steeper topography where no water accumulated during the flooding, whereas the rest was completely inundated as national quad derived DEM calculated TWIs also indicated nicely. AW3D30 and TanDEM-X DEM calculated TWIs produced similar results in visualization as well as in calculation despite the varying resolutions. However, their concentrations were mostly limited to established channel width. Dixon and Earls [46] stated that no matter how the GRID spacing was in a DEM, even if one is resampled to match another one with a specified GRID spacing, they all behave differently in hydrological studies. Bozkurt channel as experienced in many parts of the country, was in a so-called rehabilitated state, directing the water to a not-wide-enough waterway which was completely overwhelmed during the flood. Almost entire residential parts of the sub-province turned into a flood-plain, which was also apparent through the calculations done via national quad maps. Both of the quad map generated DEMs', 67 m and 104 m, visual appeal was better than the intentionally produced 30 m resampled DEM. Sorensen and Seibert [47] stated that calculated designated upstream area got smaller on average for high resolution DEMs with varying information content. Although resampled anticipating a better performance, the resulting high resolution did not necessarily produce as good of a performance as the coarser resolution ones.

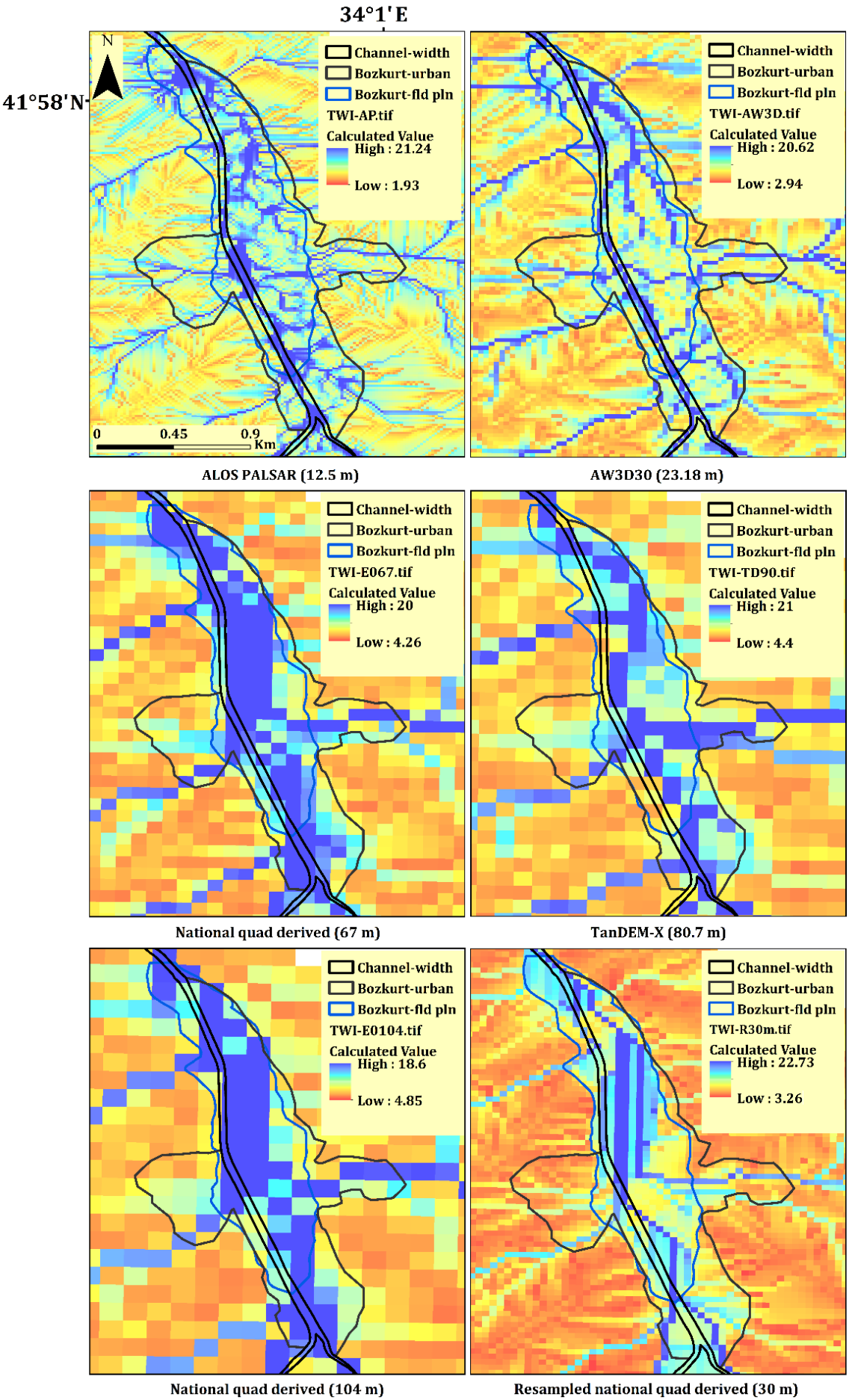

Figure 4. DEM resolution-based Bozkurt residential area inundation scenarios

Calculated TWI value-wise, all tested DEM datasets produced enough warning that a considerable part of the present-day Bozkurt sub-province residential extend will always be under flood risk unless a complete relocation of the people and infrastructure is undertaken. Besides, a comparison calculated to detect which of the tested DEMs generated approximate acreage to the heavily damaged part of the sub-province, indicated as flood plain, 60.7 ha, in Figure 4, produced the respective figures, ALOS PALSAR DEM, 13.5 ha; AW3D30 DEM, 17.2 ha; high resolution quad map derived DEM, 39.2 ha; TanDEM-X, 33.8 ha, low resolution quad map derived DEM, 46.7 ha and resampled national quad map derived DEM, 41.6 ha. Excessive detail captured with high resolution DEMs caused the results to produce rather less acreages compared to those captured with low resolution DEMs. Despite varying figures, it was obvious that quad map derived DEM variants, especially the ones generated without resampling algorithm, produced the overall best results in terms of the questioned objectives. Whether fragmented resulting from high DEM resolution, or aggregated due to low DEM resolution, TWI is a practical and valuable hydrological index for urban development strategies when new sites are planned for residential expansions or flood or landslide mitigation works.

4. Conclusion

Digital Elevation Models have become an indispensable part of the engineering works, today. Along with the technological advancements, GRID spacing is brought to unprecedented small sizes. Geoscience capabilities are also improved considerably. When one knows what to do using the data and the instrument, the results are invaluable on many matters. This simple example was applied to a feeder basin which produced record breaking flood to the town erected in lower elevations. Topographic Wetness Index algorithms calculated over different resolution DEMs showed that the threat was simply sleeping as if nothing would ever have happened. Threats must be taken seriously. Thanks to geoscience capabilities, nothing should be left unturned when lives and country's assets are at stake. Investments tied to the development phases of the cities and the well-being of the people choosing to live in them should not be taken lightly. Technology and know-how are available for the ones willing to accept and incorporate them in their planning. Thus, each and every attempt must be considered to make the living easier, more enjoyable and safer for everyone. Türkiye is not a third World country where capacity build-up is essential before the actual initiative, because financial capabilities, know-how, and trained personal are all present. More derivatives must be integrated into final decisions if they will have long term critical impacts on people's well-being. This way prosperity will thrive and ambitions will be achieved.

Acknowledgement

I thank JAXA and DLR for making the dissemination of such datasets freely accessible. I also thank Turkish General Directorate of Mapping for supplying the quad maps upon request.

Conflicts of interest

The authors declare no conflicts of interest.

References

1. Usul, N. & Turan, B. (2006). Flood forecasting and analysis within the Ulus Basin, Turkey, using geographic information systems. Natural Hazards, 39, 213-229.
2. Yuksek, O., Kankal, M. & Ucuncu, O. (2012). Assessment of big floods in the Eastern Black Sea Basin of Turkey. Environmental Monitoring and Assessment, 185, 797–814.
3. Anilan, T. & Yuksek, O. (2017). Perception of flood risk and mitigation: survey results from the Eastern Black Sea Basin, Turkey. Natural Hazards Review, 18(2), 05016006.
4. Lucà, F. & Robustelli, G. (2020). Comparison of logistic regression and neural network models in assessing geomorphic control on alluvial fan depositional processes (Calabria, southern Italy). Environmental Earth Sciences, 79, 39.
5. Hojati, M. & Mokarram, M. (2016). Determination of a topographic wetness index using high resolution digital elevation models. European Journal of Geography, 7(4), 41-52.
6. Altunel, A. O. (2018). Suitability of open-access elevation models for micro-scale watershed planning. Environmental Monitoring and Assessment, 190(9), 512.
7. Niebur, C. S., Arvidson, R. E., Guinness, E. A., & Galford, G. L. (2003). Lower Missouri River floodplain at arrow rock before and after the great floods of 1993. At the confluence: rivers, floods and water quality in the St. Louis Region, 115-134.
8. Kundzewicz, Z. W., Pińskwar, I., & Brakenridge, G. R. (2013). Large floods in Europe, 1985–2009. Hydrological Sciences Journal, 58(1), 1-7.
9. Milly, P. C. D., Wetherald, R. T., Dunne, K. A., & Delworth, T. L. (2002). Increasing risk of great floods in a changing climate. Nature, 415(6871), 514-517.
10. Dutta, D., & Herath, S. (2004). Trend of floods in Asia and flood risk management with integrated river basin approach. In Proceedings of the 2nd international conference of Asia-Pacific hydrology and water resources Association, Singapore, 1, 55-63.
11. Beven, K. J. & Kirkby, M. J. (1979). A physically based variable contributing area model of basin hydrology. Hydrological Science Bulletin, 24, 43-69.
12. Buchanan, B. P., Fleming, M., Schneider, R. L., Richards B. K., Archibald, J., Qiu, Z. & Walter, M. T. (2014). Evaluating topographic wetness indices across central New York agricultural landscapes. Hydrology and Earth System Sciences, 18, 3279-3299.
13. Ballerine, C. (2017). Topographic wetness index urban flooding awareness act action support, Will & DuPage Counties, Illinois. Illinois State Water Survey.

Available through https://www.ideals.illinois.edu/items/104004 last accessed on 07/07/2022.
14. Qin, C. Z., Zhu, A. X., Pei, T., Li, B. L., Scholten, T., Behrens, T., & Zhou, C. H. (2011). An approach to computing topographic wetness index based on maximum downslope gradient. *Precision agriculture*, *12*(1), 32-43.
15. ALOS-PALSAR. (2022). Alaska Satellite Facility (ASF) Data Search-Vertex. Available through https://search.asf.alaska.edu/#/?dataset=ALOS, last accessed on 21/04/2022.
16. AW3D30. (2022). ALOS Global Digital Surface Model "ALOS World 3D – 30m" (AW3D30). Available through https://www.eorc.jaxa.jp/ALOS/en/aw3d30/data/index.htm, last accessed on 21/04/2022.
17. TanDEM-X. (2022). TanDEM-X Digital Elevation Model (DEM)-Global 90m. Available through https://download.geoservice.dlr.de/TDM90/, last accessed on 21/04/2022.
18. Yan, S., Guo, H., Liu, G. & Ruan, Z. (2013). Mountain glacier displacement estimation using a DEM-assisted offset tracking method with ALOS/PALSAR data. Remote Sensing Letters, 4(5), 494-503.
19. Wessel, B., Huber, M., Wohlfart, C., Marschalk, U., Kosmann, D. & Roth, A. (2018). Accuracy assessment of the global TanDEM-X Digital Elevation Model with GPS data. ISPRS Journal of Photogrammetry and Remote Sensing, 139, 171-182.
20. Santillan, J. R., Makinano-Santillan, M. & Makinano, R. M. (2016). Vertical accuracy assessment of ALOS World 3D-30M Digital Elevation Model over northeastern Mindanao, Philippines. In 2016 IEEE International Geoscience and Remote Sensing Symposium (IGARSS) (pp. 5374-5377).
21. Caglar, B., Becek, K., Mekik, C. & Ozendi, M. (2018). On the vertical accuracy of the ALOS world 3D-30m digital elevation model. Remote Sensing Letters, 9(6), 607-615.
22. De Oliveira A. F. C. & De FáTima R. D. (2012). Effectiveness of SRTM and ALOS-PALSAR data for identifying morphostructural lineaments in northeastern Brazil. International Journal of Remote Sensing, 33(4), 1058-1077.
23. Senkal, E., Kaplan, G., & Avdan, U. (2021). Accuracy assessment of digital surface models from unmanned aerial vehicles' imagery on archaeological sites. International Journal of Engineering and Geosciences, 6(2), 81-89.
24. Ghosh, S. & Kundu, S. (2022). Morphometric Characterization and Erosion Assessment of Gullies in the Lateritic Badlands of Eastern India using ALOS AW3D30 DEM and Topographic Indices. *Geocarto International*, 1-34 https://doi.org/10.1080/10106049.2022.2032390
25. Pandey, P., Manickam, S., Bhattacharya, A., Ramanathan, A. L., Singh, G. & Venkataraman, G. (2017). Qualitative and quantitative assessment of TanDEM-X DEM over western Himalayan glaciated terrain. Geocarto International, 32(4), 442-454.
26. Akar, A. (2017). Evaluation of accuracy of dems obtained from uav-point clouds for different topographical areas. International Journal of Engineering and Geosciences, 2(3), 110-117.
27. Kilicoglu, A., Direnc, A., Yildiz, H., Bolme, M., Aktug, B., Simav, M. & Lenk, O. (2011). Regional gravimetric quasi-geoid model and transformation surface to national height system for Turkey (THG-09). Studia geophysica et geodaetica, 55(4), 557-578.
28. ALOS-PALSAR. (2022). ALOS PALSAR – Radiometric Terrain Correction. Available through https://asf.alaska.edu/data-sets/derived-data-sets/alos-palsar-rtc/alos-palsar-radiometric-terrain-correction/, last accessed on 25/04/2022.
29. Yilmaz, A. & Erdogan, M. (2018). Designing high resolution countrywide DEM for Turkey. International Journal of Engineering and Geosciences, 3(3), 98-107.
30. Pike, R. J., & Wilson, S. E. (1971). Elevation-relief ratio, hypsometric integral, and geomorphic area-altitude analysis. Geological Society of America Bulletin, 82(4), 1079-1084.
31. Lecordix, F., Gallic, J. L., Gondol, L., & Braun, A. (2007, August). Development of a new generalization flowline for topographic maps. In *10th ICA workshop on Generalisation and Multiple Representation* (pp. 2-3).
32. Oka, S., Garg, A. & Varghese, K. (2012). Vectorization of contour lines from scanned topographic map. Automation in Construction, 22, 192-2020.
33. Pourali, S. H., Arrowsmith, C., Chrisman, N., Matkan, A. A. & Mitchell, D. (2016). Topography wetness index application in flood-risk-based land use planning. Applied Spatial Analysis and Policy, 9(1), 39-54.
34. Aksoy, H., Kirca, V. S. O., Burgan, H. I. & Kellecioglu, D. (2016). Hydrological and hydraulic models for determination of flood-prone and flood inundation areas. Proceedings of the International Association of Hydrological Sciences, 373, 137-141.
35. Werbrouck, I., Antrop, M., Van Eetvelde, V., Stal, C., De Maeyer, P., Bats, M., ... & Zwertvaegher, A. (2011). Digital Elevation Model generation for historical landscape analysis based on LiDAR data, a case study in Flanders (Belgium). Expert Systems with Applications, 38(7), 8178-8185.
36. Bühler, Y., Marty, M. & Ginzler, C. (2012). High resolution DEM generation in high-alpine terrain using airborne remote sensing techniques. Transactions in GIS, 16(5), 635-647.
37. Tepeköylü, S. (2016). Mobil Lidar Uygulamaları, Veri İşleme Yazılımları ve Modelleri. Geomatik, 1(1), 1-7.
38. San, B. T. & Suzen, M. L. (2005). Digital elevation model (DEM) generation and accuracy assessment from ASTER stereo data. International Journal of Remote Sensing, 26(22), 5013-5027.
39. Uysal, M., Toprak, A. S. & Polat, N. (2015). DEM generation with UAV Photogrammetry and accuracy analysis in Sahitler hill. Measurement, 73, 539-543.
40. Li, J. & Wong, D. W. (2010). Effects of DEM sources on hydrologic applications. Computers, Environment and Urban Systems, 34(3), 251-261.
41. Walker, J. P. & Willgoose, G. R. (1999). On the effect of digital elevation model accuracy on hydrology and geomorphology. Water Resources Research, 35(7), 2259-2268.

42. Saksena, S., & Merwade, V. (2015). Incorporating the effect of DEM resolution and accuracy for improved flood inundation mapping. Journal of Hydrology, 530, 180-194.
43. Jeon, J. H., Ham, J. H., Chun, G. Y. & Kim, S. J. (2002). Effects of DEM Resolution on Hydrological Simulation in, BASINS-BSPF Modeling. *Magazine of the Korean Society of Agricultural Engineers, 44(7),* 25-35.
44. Hancock, G. R. (2005). The use of digital elevation models in the identification and characterization of catchments over different grid scales. Hydrological Processes: An International Journal, 19(9), 1727-1749.
45. Mohanty, M. P., Nithya, S., Nair, A. S., Indu, J., Ghosh, S., Bhatt, C. M., ... & Karmakar, S. (2020). Sensitivity of various topographic data in flood management: Implications on inundation mapping over large data-scarce regions. Journal of Hydrology, 590, 125523.
46. Dixon, B & Earls, J. (2009). Resample or Not?! Effects of resolution of DEMs in watershed modeling. *Hydrological Processes: An International Journal*, 23(12), 1714-1724.
47. Sorensen, R. & Seibert, J. (2007). Effects of DEM resolution on the calculation of topographical indices: TWI and its components. Journal of Hydrology, 347(1-2), 79-89.